Combustion synthesis of nanocrystalline ZnO powders using zinc nitrate and glycine as reactants—influence of reactant composition

CHYI-CHING HWANG*, TSUNG-YUNG WU
Department of Applied Chemistry, Chung Cheng Institute of Technology, Tashi Jen, Taoyuan 335, Taiwan
E-mail: cchwang1@ccit.edu.tw

Zinc oxide (ZnO) has a wurtzite structure, a characteristic of semi-conductors, and is used in electronic ceramic devices [1, 2] and photo catalysts [3, 4]. Nanoscale particles possess different physical and chemical properties compared to bulk materials. Better sinterability, higher catalytic activity, and other unique properties may be expected because of their nano-sized crystallite, large surface area and different surface properties (such as surface defect), etc. At present, two methods are generally being used to obtain nanosized ZnO powder: vapor method and sol-gel method, which require high processing and chemicals costs, respectively [5], Therefore, the synthesis method of nano-sized ZnO powders can still be improved.

Recently, several researchers proposed the solution combustion method to synthesize simple and mixed metal oxides [6–11]. Using this method, the heating and evaporation of metal nitrate solution with an organic compound (such as glycine, urea, or citric acid etc.) results in self-firing and generates intense heat by exothermic reaction. This intense heat is used to synthesize the ceramic powders. This novel approach has the advantages of inexpensive raw materials, a relatively simple preparation process, and a fine resulting powder with high homogeneity. Although there is little literature reporting that nanosized ZnO have been synthesized by this method [4, 5, 12, 13], there is also hardly any information available on the effects of reactant composition in the nature of combustion reaction phenomena on the properties of as-synthesized ZnO powders. In this work, the study of correlation among reactant composition, reaction phenomena, and product characteristics are undertaken.

Glycine (NH_2CH_2COOH) was selected as the fuel since it is inexpensive and its combustion heat (-3.24 Kcal/g) is more negative when compared with urea (-2.98 Kcal/g) or citric acid (-2.76 Kcal/g). On the other hand, zinc nitrate [$Zn(NO_3)_2{\cdot}6H_2O$] is utilized in the present work because of its dual role of being the zinc source and the oxidant. The combustion reaction can be expressed (but over-simplified) as follows:

$$Zn(NO_3)_2{\cdot}6H_2O_{(c)} + \psi NH_2CH_2COOH_{(c)} + (2.25\psi - 2.5)O_{2(g)} \xrightarrow{\Delta} ZnO_{(c)} + (1 + 0.5\psi)N_{2(g)} + 2\psi CO_{2(g)} + (6 + 2.5\psi)H_2O_{(g)} \quad ((7.5 + 2.75\psi) \text{ moles gases produced}) \quad (1)$$

where ψ is defined as the molar ratio of glycine-to-zinc nitrate. Note that $\psi = 1.11$ corresponds to the situation of an 'equivalent stoichiometric ratio,' which implies that the oxygen content of zinc nitrate can be completely reacted to oxidize/consume glycine exactly. As a result, ZnO product and gases of CO_2, H_2O and N_2 can be formed directly from the reaction between fuel and oxidizer without the necessity of getting oxygen from outside.

In this work, the ZnO was synthesized by an amount of 25 grams per batch according to the flow chart shown in Fig. 1. Analytic grade zinc nitrate and glycine were directly mixed at a desired molar ratio without adding water. (In our opinion, it is appropriate to omit the procedure of dissolving the reactants in water to form a solution.) From our experiment, it was found that zinc nitrate possesses hygroscopicity. The reactant mixture easily absorbed moisture from the air to become a transparent slurry mixture, which was heated on a hot-plate and thoroughly dehydrated. The dried mixture (hereafter termed as precursor) possesses the characteristic of combustion, and can be ignited to start combustion reaction by using a mini gas burner at room temperature. On doing so, combustion of the precursor with the evolution of a large volume of gases occurs, producing a loose product. It was found that the nature of the combustion and the characteristics of the as-synthesized product depend on the ψ value (see below for details).

Thermogravimetric (TG) and differential thermal analysis (DTA) of the precursor were carried out at a heating rate of 10 °C/min in static air (TA Instruments, SDT 2960, USA). The maximum combustion temperature (T_c) reached was measured by using a S-type (Pt/Pt-10%Rh) thermocouple. Phase formation of the product was identified by using X-ray diffraction (XRD) (SIEMENS D5000, Germany) with Cu K_α radiation. The morphological features of the product were imaged by transmission electronic microscope (TEM) (Hitachi H-7100, Japan). Powder surface area was measured using the single point BET nitrogen adsorption method (Micromeritics, ASAP 2010, USA). Perkin-Elmer CHN elemental analyzer (Model: 2400(II),

*Author to whom all correspondence should be addressed.

0022–2461

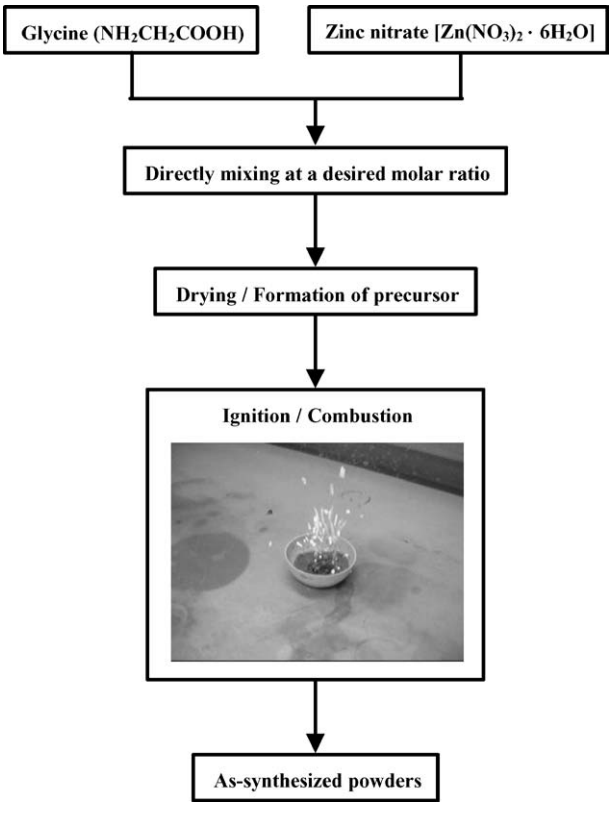

Figure 1 Flow chart for synthesis of ZnO using this proposed combustion method.

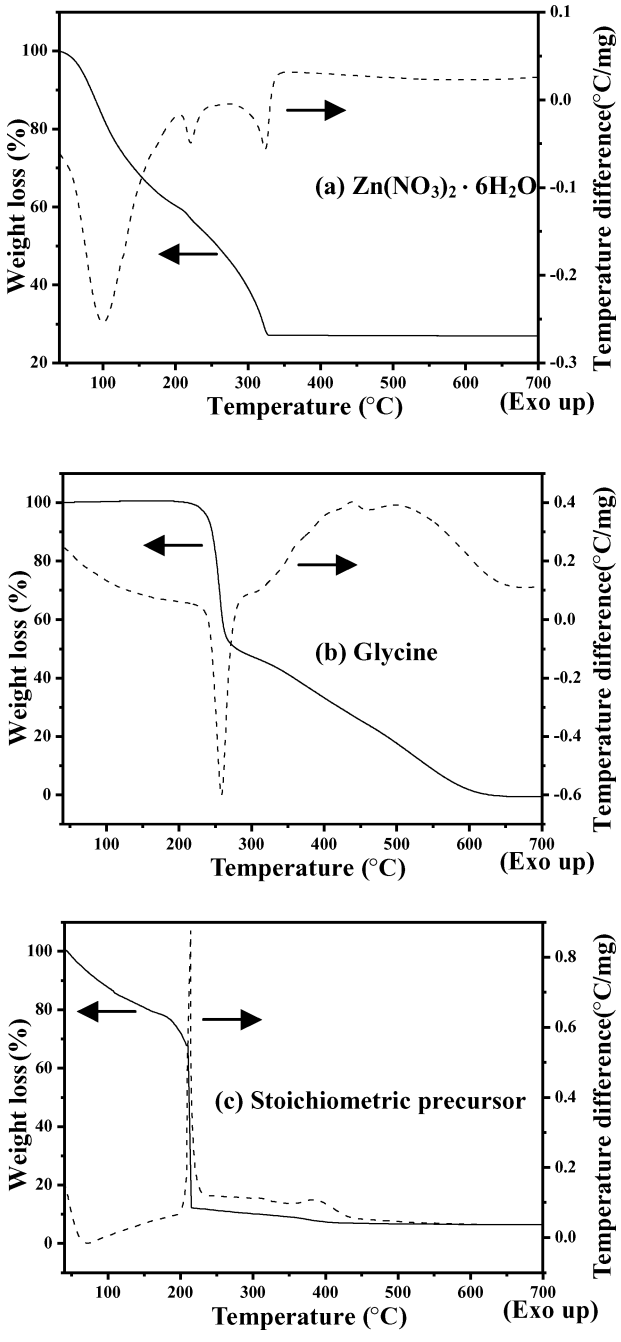

Figure 2 Typical TG–DTA curves of the (a) $Zn(NO_3)_2{\cdot}6H_2O$, (b) glycine (NH_2CH_2COOH), and (c) stoichiometric precursor.

USA) was employed to measure the content of residual carbon.

The simultaneous TG-DTA curves of the stoichiometric precursor (i.e., $\psi = 1.11$) and its ingredients are shown in Fig. 2. Judging from the results of TG analysis, $Zn(NO_3)2{\cdot}6H_2O$ can be decomposed completely into ZnO below 330 °C (Fig. 2a). However, the residue (i.e., ZnO) is amorphous in nature as identified by XRD shown in Fig. 3. For pure glycine, the results of TG-DTA (Fig. 2b) show that the exothermic reaction takes place between 266–640 °C accompanied with weight loss from 47 to 100%, corresponding to the complete oxidation of carbonaceous matter. As shown in Fig. 2c, the decomposition of the precursor occurs suddenly in a single step. The strongly exothermic behavior of decomposition can be clearly seen at about 210 °C. The maximum weight loss occurs in a very narrow temperature range, which corresponds to the decomposition step. The observed weight loss associated with this exothermic reaction is approximately 56%. By comparing the TG-DTA curves of the precursor and its ingredients, it is suggested that the acceleration of the reaction rate (i.e., the slope of weight loss-temperature curve is very steep) and the lowering of the decomposition temperature may be attributed to the presence of nitrate ion in the precursor since the NO_3-ions provide an *in situ* oxidizing environment for the oxidation of the organic component. The combination of the lowering of the reaction temperature and the increase in reaction rate result in a combustion reaction of the glycine-nitrate precursor.

In order to understand the variation in adiabatic flame temperature (T_{ad}) with the molar ratio of glycine-to-zinc nitrate (ψ), the T_{ad} could be calculated theoretically for various molar ratios. Thermodynamic data [14, 15] of various reactants and products, which are available from the literature are listed in Table I. The enthalpy of reaction can be expressed as:

$$\Delta H^\circ = \left(\sum n \cdot \Delta H_f^\circ\right)_{\text{products}} - \left(\sum n \cdot \Delta H_f^\circ\right)_{\text{reactants}} \quad (2)$$

where n is the number of the mole. Using the thermodynamic data for various reactants and products listed in Table I, the enthalpy of reaction for Equation 1 as a function of the ψ value can be determined as follows:

$$\Delta H^\circ = 120.904 + \psi(-252.882) \quad (25\,^\circ\text{C, Kcal}) \quad (3)$$

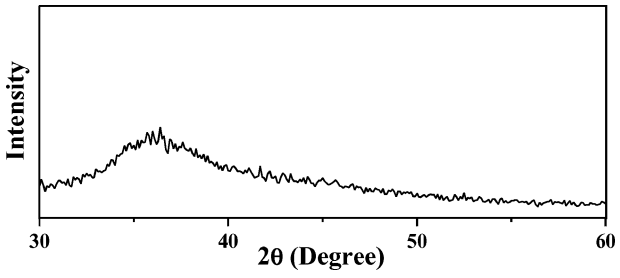

Figure 3 XRD pattern of the product obtained by using $Zn(NO_3)_2{\cdot}6H_2O$ calcined at 330 °C.

The following equation can be used to theoretically approximate the adiabatic flame temperature for a combustion reaction:

$$Q = -\Delta \mathrm{H}^\circ = \int_{298}^{\mathrm{Tad}} \left(\sum n \cdot c_\mathrm{p} \right)_{\mathrm{products}} \mathrm{d}T \quad (4)$$

where Q is the heat absorbed by products under adiabatic condition, and c_p is the heat capacity of the products at constant pressure. Substituting the thermodynamic data from Table I and Equation 3 into Equation 4, the adiabatic flame temperature (T_ad) for the combustion reaction between glycine and zinc nitrate with various ψ values can be calculated. The variation of the T_ad versus the ψ value is shown in Fig. 4. As expected, it increases substantially with the amount of fuel used during combustion.

The plot of the maximum combustion temperature (T_c) as a function of the ψ value together with the characteristic combustion regimes are shown in Fig. 4. The measured values of T_c are typically lower than the calculated values of T_ad due to heat loss. The T_c increases with increasing ψ value to a maximum of ~1250 °C (at $\psi = 1.5$) and then decreases with further increase in the molar ratio.

TABLE I Relevant thermodynamic data

Compound[a]	$\Delta H_\mathrm{f}^\mathrm{o}$ (Kcal/mol)	C_p (Kcal/mol · K)
$Zn(NO_3)_2{\cdot}6H_2O_{(c)}$	−550.92	0.0722
$NH_2CH_2COOH_{(c)}$	−79.71	$0.019 + 0.00131T^b$
$ZnO_{(c)}$	−83.24	0.00962
$O_{2(g)}$	0	14.73
$N_{2(g)}$	0	$5.92 + 0.00367T^b$
$CO_{2(g)}$	−94.051	$6.50 + 0.0010T^b$
$H_2O_{(g)}$	−57.796	$10.34 + 0.00274T^b$

[a](c) = Crystalline, (g) = Gas.
[b]T = Absolute temperature.

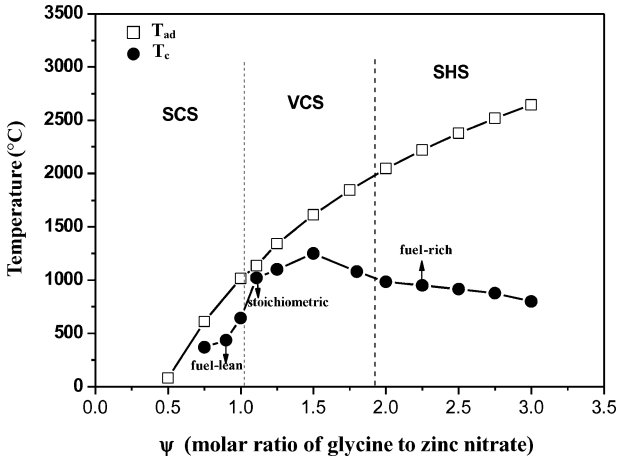

Figure 4 Adiabatic flame temperature (T_ad) and maximum combustion temperature (T_c) achieved for different combustion mode as a function of the molar ratio of glycine-to-zinc nitrate (ψ).

As noted above, depending on ψ, the reaction can proceed in three different modes:

1. Smoldering Combustion Synthesis (SCS), $\psi < 1.05$, with maximum combustion temperature, $T_\mathrm{c} < 650$ °C;
2. Volume Combustion Synthesis (VCS), $1.05 < \psi < 1.90$, 1000 °C $< T_\mathrm{c} <$ 1250 °C;
3. Self-propagating High-temperature Synthesis (SHS), $1.90 < \psi < 3.00$, 850 °C $< T_\mathrm{c} <$ 1000 °C.

SCS mode is characterized by a relatively slow, essentially flameless, reaction. Since the fuel content is small, the heat evolved is not enough and thus the temperature is lower. This leads to slower reaction rates as manifested in the smoldering combustion behavior. Moreover, it was experimentally observed that below the ψ value of 0.75, combustion reaction ceases to occur. In this regime, the ψ value of 0.90 represents a fuel-lean ratio. Extremely fast reaction characterizes the VCS mode. In this case, it is important that the reaction occurs simultaneously in the reaction volume, since the fuel-to-oxidant ratio is within a proper range ($1.05 < \psi < 1.90$), while the oxygen content contained in the precursor is the main source of oxygen required for combustion reaction. Once oxygen, which comes from NO_3^-, is generated, it immediately reacts with glycine and oxidizes/consumes most of the fuel, and thus results in the phenomenon of VCS reaction. Finally, the characteristic feature of the SHS mode is that

TABLE II Effects of molar ratio of glycine-to-zinc nitrate (ψ) on nature of combustion and characteristics of as-synthesized products

ψ	Reaction mode	T_ad[a] (°)	T_c[b] (°)	Amount of gases produced[c] (mole)	Crystallite size[d] (nm)	Specific surface area (m^2/g)	Carbon content (wt%)
0.90 (fuel-lean)	SCS	855	435	9.98	47.2	20.8	4.26
1.11 (stoichiometric)	VCS	1135	1020	10.55	60.3	17.6	0.85
2.25 (fuel-rich)	SHS	2220	950	13.69	35.6	31.5	0.91

[a]Calculated theoretically by thermodynamic data and Equation 4.
[b]Measure by using Pt-Pt/10%Rh thermocouple.
[c]Obtained from Equation 1.
[d]Estimated by Scherer formula (X-ray line broadening).

reaction initiates locally and propagates as a combustion wave in a self-sustained manner through the reaction volume. When there is excess fuel, the combustion reaction needs oxygen supplied externally. Oxygen enters through diffusion into the reaction zone by kinetic factors which limit the reaction rate and, eventually, the SHS reaction mode. In this regime, the ψ value of 2.25 was selected as a representative of fuel-rich ratio.

Fig. 5 shows the XRD patterns of the as-synthesized powders prepared at three different molar ratios of glycine-to-zinc nitrate (i.e., $\psi = 0.90$, 1.11 and 2.25). As can be seen in Fig. 5a, the relatively low signal/noise ratio and some unknown diffraction peaks indicate that the as-synthesized powder prepared using $\psi = 0.90$ (fuel-lean, SCS mode) consists of insufficiently developed crystalline ZnO and impurities because the inadequate fuel could not react completely with the zinc nitrate to release enough heat to form the well-developed phase of ZnO. However, when $\psi = 1.11$ (stoichiometric, VCS mode) or $\psi = 2.25$ (fuel-rich, SHS mode) was used, the product seemed to contain single-phased ZnO because only the characteristic peaks of ZnO were observed (Fig. 5b and c).

Table II shows the characteristics of the as-synthesized powder prepared at three different fuel-to-oxidant molar ratios ($\phi = 0.90$, 1.11 and 2.25). The grain size of the as-synthesized product was estimated according to the Scherer formula [16]. It was found that all the products obtained in this work are nanocrystallites with the sizes ranging between 34 and 75 nm. Also, their surface areas are large (~18–32 m^2/g), and the as-synthesized powder obtained through the fuel-rich precursor has the largest specific surface area as compared with that of stoichiometric and fuel-lean precursors. The carbon contents of the as-synthesized product with $\psi = 0.90$ is relatively high as compared with that using $\psi = 1.11$ and 2.25. This result, coupled with its XRD spectrum being detected to include impurity

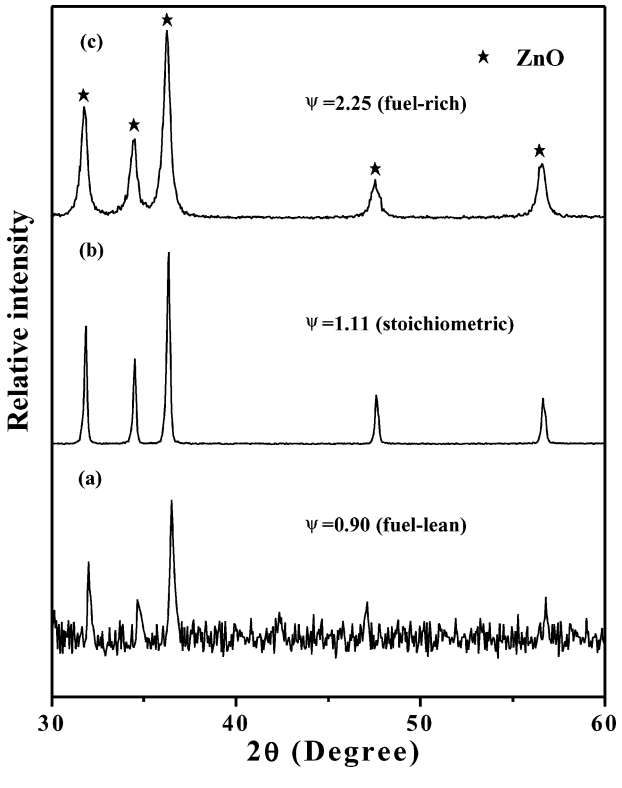

Figure 5 XRD patterns of the as-synthesized product with different molar ratio of glycine-to-zinc nitrate: (a) $\psi = 0.90$ (fuel-lean), (b) $\psi = 1.11$ (stoichiometric), and (c) $\psi = 2.25$ (fuel-rich).

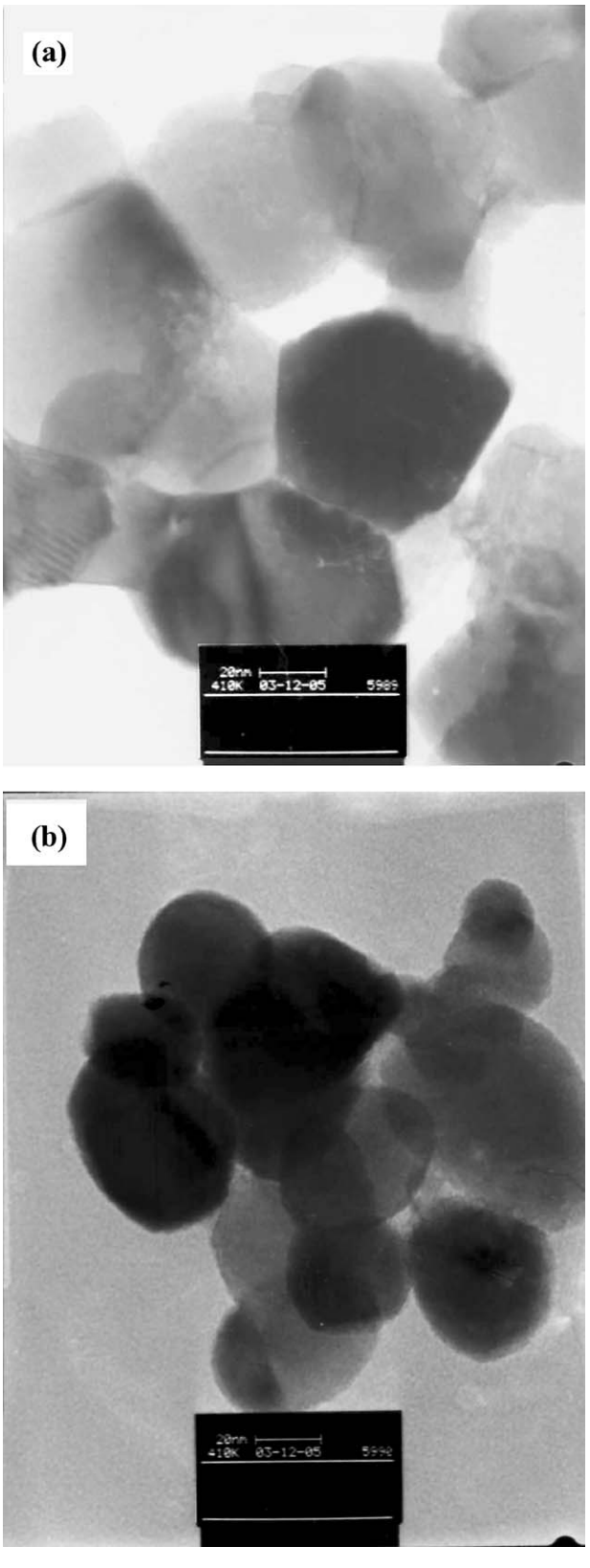

Figure 6 TEM photographs of the ZnO powder obtained through: (a) the stoichiometric, and (b) the fuel-rich precursors (taken at the same magnification of ×410,000).

(Fig. 5a), which is attributed to the heat released during combustion, is relatively low for the fuel-lean precursor. Hence, the local temperature reaction zone remains low (∼435 °C, see Fig. 4), causing the combustion reaction to be incomplete.

High combustion temperature can adversely affect powder characteristics such as an increase in the crystallite size and premature local partial sintering among the active primary particles produced during reaction, thereby reducing the specific surface area. The differences in particle size and the combustion temperature with the use of different ψ values may also depend on the mole number of gaseous products. As more gases are liberated, the agglomerates disintegrate and additional heat is carried from the system thereby hindering particle growth, which may produce powder with a high specific surface area. As seen from Equation 1, the total mole number of gaseous products increases with the increasing of ψ value. Possibly, there could be competition between the effect of the combustion temperature and the number of moles of the evolved gases in influencing the specific surface area of the powder product. Our results tend to indicate that the latter plays a more dominant role since the specific surface area is larger for the ZnO powder obtained through the fuel-rich precursor as compared to that of the stoichiometric and fuel-lean precursors.

The TEM photographs were taken after the VCS and SHS products ($\psi = 1.11$ and 2.25) had been fully ground and were treated with oscillation procedures. Fig. 6a and b show the typical TEM photographs of nearly hexagonal nanocrystalline ZnO particles with which to confirm the lower particle size distribution in the case of fuel-rich ratio in comparison with the stoichiometric ratio. Furthermore, the crystallite sizes measured by TEM for the ZnO particles obtained through the stoichiometric and fuel-rich precursors respectively, are ∼50 and ∼30 nm, which are about the same sizes as estimated by using XRD method.

Explorations of the sintering behavior, microstructure, and electronic properties of the doped-ZnO prepared by this method are underway and we will soon disclose where we stand.

Acknowledgment

Support for this research by the National Science Council of the Republic of China under grant no. NSC 91-2214-E-014-002 is gratefully acknowledged.

References

1. T. K. GUPTA, "Influence of Microstructure and Chemistry on the Electrical Characteristics of ZnO Varistors," in Tailoring Multiphase and Composite Ceramics, edited by R. E. Tressler, G. L. Messing, C. G. Pantino and R. H. Newhan (Plenum, New York, 1986) p. 439.
2. R. WU, C. XIE, H. XIA, J. HU and A. WANG, *J. Cryst. Growth* **217** (2000) 274.
3. R. J. FARRAUTO and R. M. HECK, *Catal. Today* **55** (2000) 179.
4. K. R. LEE, S. PARK, K. W. LEE and J. H. LEE, *J. Mater. Sci. Lett*. **22** (2003) 65.
5. C. R. LEE, H. W. LEE, J. S. SONG, W. W. KIM and S. PARK, *J. Mater. Synth. Proc.* **9** (2001) 281.
6. L. A. CHICK, L. R. PEDERSON, G. D. MAUPIN, J. L. BATES, L. E. THOMAS and G. J. EXARHOS, *Mater. Lett.* **10** (1990) 6.
7. L. E. SHEA, J. MCKITTRICK, O. A. LOPEZ and E. SLUZKY, *J. Amer. Ceram. Soc.* **79** (1996) 3257.
8. H. C. SHIN, K. R. LEE, C. H. JUNG, S. J. KIM and S. PARK, *Jpn. J. Appl. Phys.* **35** (1996) L996.
9. R. D. PUROHIT, B. P. SHARMA, K. T. PILLAI and A. K. TYAGI, *Mater. Res. Bull.* **36** (2001) 2711.
10. T. MIMANI and K. C. PATIL, *Mater. Phys. Mech.* **4** (2001) 134.
11. F. LI, K. HU, J. LI, D. ZHANG and G. CHEN, *J. Nucl. Mater.* **300** (2002) 88.
12. V. C. SOUSA, A. M. SEGADAES, M. R. MORELLI and R. H. G. A. KIMINAMI, *Intern. J. Inorg. Mater.* **1** (1999) 235.
13. V. C. SOUSA, M. R. MORELLI, R. H. G. A. KIMINAMI and M. S. CASTRO, *J. Mater. Sci.* **13** (2002) 319.
14. R. H. PERRY and C. H. CHILTON, "Chemical Engineering Handbook", 7th ed. (McGraw-Hill, New York, 1997).
15. J. A. DEAN (ed.), "Lange's Handbook of Chemistry", 15th ed. (McGraw-Hill, New York, 1998).
16. H. P. KLUG and L. E. ALEXANDER, "X-ray Diffraction Procedures for Polycrystalline and Amorphous Materials" (Wiley, New York, NY, 1997) p. 637.

Received 5 March
and accepted 21 April 2004